

Research Journal of Pharmaceutical, Biological and Chemical Sciences

TiO₂-SiO₂ mixed oxides: Xerogel catalyst for the Selective Epoxidation of cyclohexene

Ilhem Rekkab-Hammoumraoui, Ilyes Khaldi, Abderrahim Choukchou-Braham* and Redouane Bachir

Laboratoire de Catalyse et Synthèse en Chimie Organique, Faculté des sciences, Université de Tlemcen, Algeria.

ABSTRACT

A porous TiO₂-SiO₂ mixed metal oxide was synthesized via sol-gel route using inorganic precursors and subsequently dried, and then calcined at different temperatures (250, 400 and 600 °C). The mixed oxide was characterized by XRD, as well as by FTIR and diffuse reflectance ultraviolet-visible (DRS-UV-vis). The hydrophobicity (H) and relative abundance of Ti-O-Si linkages or Ti dispersion (D, T) were calculated. The catalysts were evaluated in the cyclohexene epoxidation with TBHP (^{tert}-butyl hydroperoxide) as oxidant agent; the selectivity toward cyclohexene epoxide was 100 % and the conversion was 44 %. The effects of varying the catalyst calcination temperature and adding slowly the oxidant and solvent were investigated. The catalytic data obtained showed that the activity can be influenced by the coordination environment of titanium species. The insights obtained from these studies allowed a fundamental understanding of the relationships between the structural characteristics and the physicochemical/reactivity properties of titania-silica catalysts.

Keywords: Titanium-silica catalysts, Sol-gel, Hydrophobicity, Dispersion, Epoxidation, Cyclohexene, TBHP.

**Corresponding author*

INTRODUCTION

The preparation of supports and heterogeneous catalysts by sol-gel processing has increasingly attracted interest in recent years. Sol-gel processing allows the formation of oxides with controlled porosity and shape (coatings, fibers, powders, monoliths). It is particularly useful for the preparation of multi component oxides with a high degree of homogeneity [1 – 3]. Actually, the ability of sol-gel to form mixed M–O–M' bonds (where M and M' denote two different metal atoms) leads to high densities of acid sites, while providing the high surface area and high pore volume desirable for catalytic applications [4]. Titania–silica mixed oxides are active and selective epoxidation catalysts [5 - 7], offering an efficient alternative to the conventional titania-on-silica and Ti-substituted zeolites. Mixed oxides are usually synthesized by the sol-gel method. Despite the substantial effort in the past years, a comprehensive picture of the real nature of active sites in titania–silica has not been found. The main reason is the complexity of these materials: Unlike TS-1, amorphous aerogels and xerogels present various structures [8, 9]. These structures evolve during the sol-gel synthesis according to the reactivity of precursors and their conditions; and a remarkable restructuring may occur in the subsequent aging, drying, and calcinations steps. Two types of titania–silica catalysts have been intensively investigated: silica-supported titania (Shell catalyst) [10] and mesoporous titania–silica mixed oxides [11, 12]. Titania–silica mixed oxides based on the sol-gel method [2] may exhibit better titanium distribution throughout the silica matrix when compared to the Shell catalyst.

Recently, fine-chemical industry has pointed out that olefin epoxidation is one of the most important reactions in industrial organic synthesis. The epoxidation of olefins such as ethylene, propylene and cyclohexene, leads to the formation of oxygenated molecules called epoxides, which are very valuable and versatile intermediates for many industrial applications [13]. So far, cyclohexene epoxidation has been extensively investigated, using a large number of homogeneous catalysts which are difficult to separate from other components of the reaction medium and whose recovery is difficult. Therefore, significant efforts have been made for the development of new catalysts for the synthesis of epoxides in a more environmental friendly way [14 - 19].

TBHP is one of the industrially preferred oxygen sources for epoxidation reactions; it is a mild and selective oxidant, neither corrosive nor hazardous, and the by-product obtained from the reaction, ^{tert}-butyl alcohol, can be separated and recycled for use in other industrial processes [20]. In this work, epoxidation of cyclohexene using TBHP over 2 %TiO₂-SiO₂ was investigated using several techniques, such as diffuse reflectance ultraviolet visible (DRS-UV-vis) and Fourier transform-infrared (FT-IR) in order to understand the progress of this reaction. It is commonly accepted that, by analogy with TS-1, good activity and selectivity of the epoxidation reaction require a high abundance of tetrahedral titanium sites which are isolated by SiO "ligands" and act as Lewis acidic centres to activate the peroxide [12, 21, 22]. Octahedral Ti in titania nanodomains diminishes the catalytic performance.

Both techniques have been used in the present study aiming at refining our understanding of the structure–activity–selectivity relationship in titania–silica catalyzed epoxidation reactions.

EXPERIMENTAL

Catalyst preparation

Starting materials

Titanium tetraisopropoxide ($\text{Ti}[\text{OCH}(\text{CH}_3)_2]_4$ TIPT; Aldrich, 97 %); Tetraethylorthosilicate ($\text{Si}(\text{OC}_2\text{H}_5)_4$ TEOS, Aldrich, 98 %); Ethanol (Riedel-de Haen, 99.8 %); Chlorydric acid (Sigma-Aldrich, 36.5 %); Cyclohexene (Aldrich, 99 %); Heptane (Cheminova, 95 %); Teriobutanol (Aldrich, 99 %); Acetonitrile (Riedel-de Haen, 99.5 %) and tertibutyl hydroperoxide (TBHP, Aldrich, 70 % in water).

Catalyst preparation

The mixed oxide 2 % TiO_2 - SiO_2 was prepared by an acid-catalyzed sol-gel process [23]. Firstly, 11.03 mL (4.48 mmol) of tetraethylorthosilicate (TEOS) were dissolved in ethanol (8.78 mL), then 0.46 mL (1.49 mmol) of titanium tetraisopropoxide (TIPT) were added under stirring. Secondly, an acid solution (2.55 mL of HCl (8 N) in 1.17 mL distilled water) was added dropwise to the solution while stirring. The obtained yellow sol was aged in a beaker covered with a parafilm for 5 days. Finally, the obtained xerogel was dried at 65 °C for 5 h and calcined at different temperatures (250, 400 and 600 °C) for 5 h in air (6 °C min^{-1}).

Catalysts characterization

Diffractograms of the catalysts were obtained in X-ray diffraction (XRD) experiments performed on a Philips PW 1710 powder diffractometer using Cu $K\alpha$ radiation ($\lambda = 0.15186$ nm) and a backmonochromator. The XRD patterns were recorded using a 2 s dwell time, 0.04° step size and a constant divergence slit of 18. The crystalline planes were identified by comparison with PDF standards from ICDD.

The FT-IR spectra of the solid samples were recorded using an Agilent Technologies Cary 60 series FT-IR spectrometer, with pellet samples, with a measuring range of 400–4000 cm^{-1} . The diffuse reflectance spectra of the samples studied were recorded in the range 200–800 nm, at room temperature after drying, using a UV-Vis spectrophotometer (Perkin Elmer Lambda 800) equipped with an integration sphere. KBr was used as a reference in all cases for the dilution of the samples which exhibited extremely high absorbance.

The acidity of samples was characterized by pyridine adsorption followed by IR spectroscopy. The IR spectra were recorded on a Nicolet Magna IR spectrometer using a thin wafer (16 mm in diameter, 10–15 $\text{mg}\cdot\text{cm}^{-2}$) activated in situ in the IR cell under secondary vacuum (10^{-3} Pa) at 200 °C for 2 h. Pyridine was adsorbed on the sample at 150 °C. The IR spectra were recorded at room temperature, after activation and pyridine thermodesorption, under vacuum (10^{-3} Pa) for 1 h at 150 °C. The total amounts of Lewis acid sites accessible to pyridine were quantified by subtraction between P_{150} spectrum (spectrum of the catalyst after adsorption –desorption of pyridine at 150 °C) and P_{ref} (spectrum of the catalyst before adsorption of pyridine). This technique allowed, on one hand, the elimination of the solid intrinsic absorbance in the wavelength range considered and, on another hand,

the ignorance of the pyridine physisorption influence (below 150 °C). The concentrations of Lewis acid sites capable to retain the pyridine adsorbed at 150 °C were determined from the normalized absorbance areas of the band at 1455 cm^{-1} (PyL), using the extinction coefficients previously determined. The spectra were also recorded after pyridine thermodesorption under vacuum (10^{-3} Pa) for 1 h at 250 °C, 350 °C and 450 °C.

Catalytic activity evaluation

Catalysts were evaluated in cyclohexene epoxidation, using *tert*-butyl hydroperoxyde (TBHP) as oxidizer. Cyclohexene oxidation reactions were carried out in a 100 mL three-necked flask, placed in a temperature-equilibrated water bath and fitted with a reflux condenser. Typically, a mixture containing 12.58 mmol (1.8 mL) of TBHP, 37.5 mmol (4 mL) of cyclohexene, 3.8 mL of solvent was magnetically stirred under atmospheric pressure at 70 °C and then 150 mg of 2 wt% TiO_2 - SiO_2 catalyst was added (time zero). Some of the catalysts were also tested under the same conditions with slow addition of TBHP using a syringe pump.

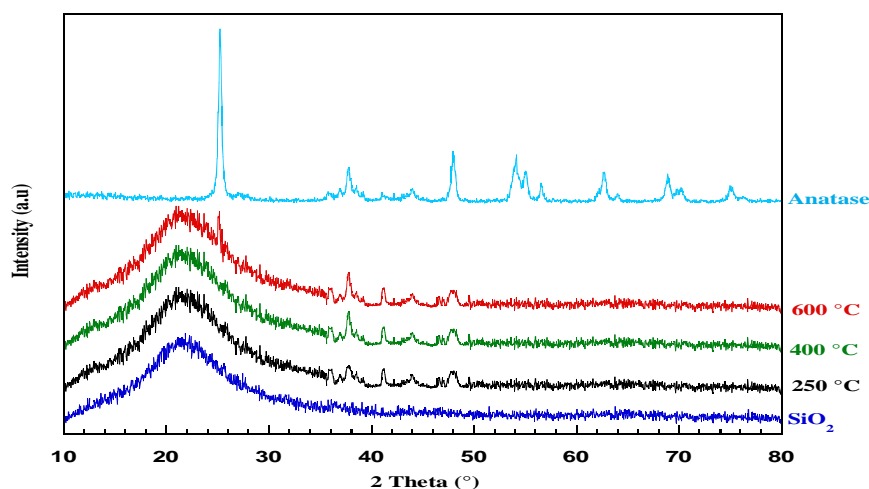
The reaction mixture was analyzed by gas chromatography (GC), taking aliquots at different reaction times. A SHIMADZU (GC-14 B) gas chromatograph equipped with a CP-wax-52 B column and a flame ionization detector (FID) was used.

Yield (%) = (moles of epoxide/moles of initial substrate) \times 100

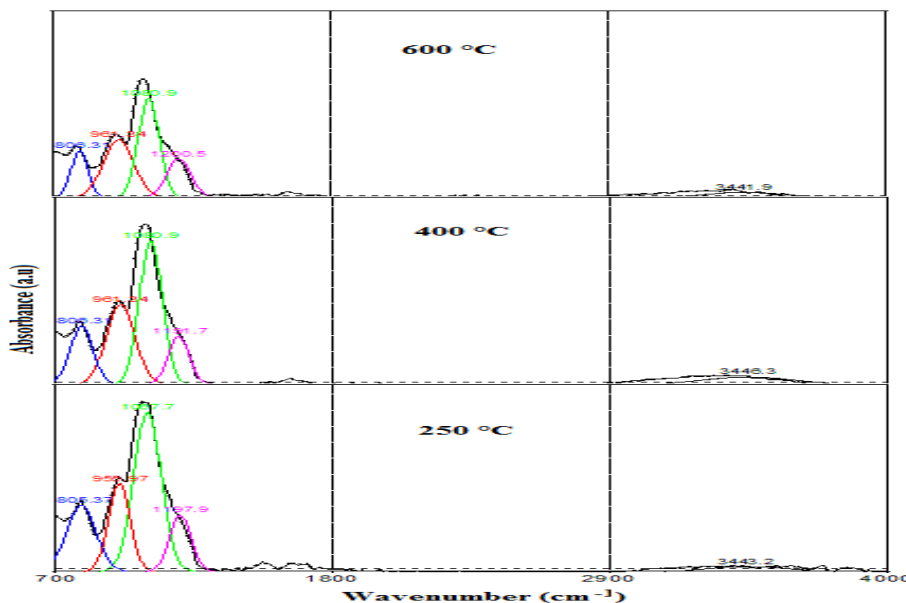
RESULTS AND DISCUSSION

Characterization

The XRD patterns of the 2 wt.% TiO_2 - SiO_2 samples are presented in Fig. 1. Spectra of all catalysts display a wide peak centred at $2\theta = 22^\circ$, characteristic of a quite amorphous SiO_2 specimen. Low-diffraction peaks, located at $2\theta = 37^\circ$, 48° and 62° corresponding to TiO_2 anatase phase, are also shown. As the calcination temperature of catalysts was increased to 600 °C, the intensity of these weaker peaks became stronger, implying that the crystallinity was enhanced.



The FTIR spectra of TiO_2 - SiO_2 catalysts prepared in this study after calcination showed the following signals (Fig. 2):



- A large band with a maximum at $\sim 3440 \text{ cm}^{-1}$ [24, 25] is attributed to the OH elongation mode of H_2O .
- A peak at $\sim 1100 \text{ cm}^{-1}$ [26] attributed to the asymmetric vibrational Si–O–Si stretching, characteristic of SiO_4 units with tetrahedral coordination; a shoulder at 1200 cm^{-1} [26], due to the asymmetric vibrational Si–O–Si stretching.
- A peak at $\sim 800 \text{ cm}^{-1}$ [2, 26] due to the corresponding symmetric vibrational Si–O–Si stretching.
- A peak at $\sim 960 \text{ cm}^{-1}$ [27] characteristic of a symmetric vibrational Si–O–Ti stretching.

The last resulting peak is crucial in determining the dispersion of TiO_2 over the silica surface, at least from a semi-quantitative point of view. In fact, it is possible to estimate the catalyst dispersion by comparing the area of the band at $\sim 960 \text{ cm}^{-1}$ with the one at $\sim 1200 \text{ cm}^{-1}$. The ratio between the two mentioned areas, $A_{(\text{Si-O-Ti})}$ and $A_{(\text{Si-O-Si})}$, calculated by a Gaussian deconvolution of the peaks, could be an index of the catalyst's dispersion [28]. The estimate of the Si-O-Ti connectivity (Ti dispersion), $D(\text{Si-O-Ti})$, is defined as:

$$D_{(\text{Si-O-Ti})} = \frac{S_{(\text{Si-O-Ti})}}{S_{(\text{Si-O-Si})}} * \frac{X_{\text{Si}}}{X_{\text{Ti}}} \quad (1)$$

$S_{(\text{Si-O-Ti})}$ and $S_{(\text{Si-O-Si})}$ are the deconvoluted peak areas of the $\nu(\text{Si-O-Ti})$ band at 960 cm^{-1} and the $\nu(\text{Si-O-Si})$ band at 1200 cm^{-1} ; X_{Si} and X_{Ti} designate the molar proportions of Si and Ti, respectively. Such $D_{(\text{Si-O-Ti})}$ values represent a semi-quantitative measure of the proportion of Si-O-Ti species referring to the total Ti content, and thus a kind of mixing efficiency or estimate of Ti dispersion.

In this paper a new measure of the hydrophobic index (H) is suggested. The best characterization is probably obtained from the deconvoluted peak areas of the $\nu(\text{Si-O-Si})$

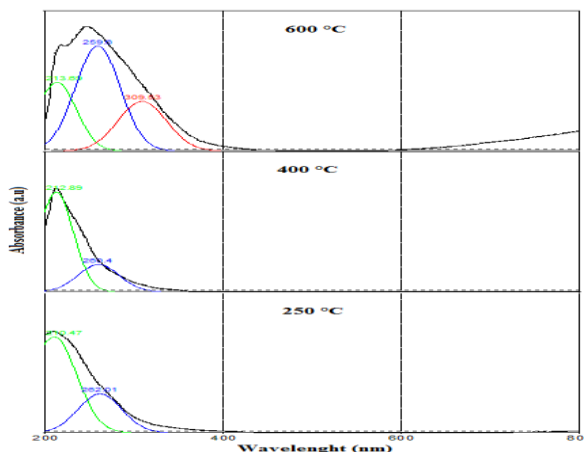
band at 1200 cm^{-1} and that of the OH group at 3440 cm^{-1} . The hydrophobic index (H) is defined as:

$$H = \frac{S_{(Si-O-Si)}}{S_{(-O-H)}} \quad (2)$$

The mixed metal oxides $\text{TiO}_2\text{-SiO}_2$ were submitted to DR-UV analysis in order to provide information about the coordination geometry of the Ti cations. The DR-UV-vis spectra of all prepared samples are compared in Fig. 3. The spectrum of bulk TiO_2 (anatase) is also included in the figure for a useful comparison. The absorption of silica in the range 200–500 nm can be considered negligible. It is well known that the Ti cations in tetrahedral coordination show a typical band at $\sim 212\text{ nm}$, due to the ligand-metal charge transfer between Ti^{4+} and oxygen ligands, such as $-\text{O}-\text{H}$, $-\text{O}-\text{Si}$, $-\text{O}-\text{Ti}$, or H_2O . On the other hand, a shift of the band towards higher wavelengths ($\sim 260\text{ nm}$) is usually observed for the Ti cations in octahedral environments. The DR-UV-vis spectra of the three catalysts calcined at $250\text{ }^\circ\text{C}$, $400\text{ }^\circ\text{C}$ and $600\text{ }^\circ\text{C}$, showed an absorption band at 210 nm , attributed to isolated Ti(IV) species in tetrahedral coordination [29 – 38]. Another band appears at 260 nm for the catalyst calcined at $600\text{ }^\circ\text{C}$, attributed to Ti (IV) species in octahedral coordination [39]. Furthermore, the samples showed a broad absorption band with a shape very similar to that of bulk anatase TiO_2 . This result suggests that, even though the TiO_2 crystallites are very small and beyond the detection sensitivity of XRD measurements, they may still possess the same electronic properties as the pure TiO_2 anatase phase.

However, the deconvoluted spectra of all catalysts showed an absorption band at 260 nm , indicating the presence of octahedral titanium (Fig. 3). Otherwise, a new method is suggested to estimate the catalyst's dispersion, the ratio (T) using the areas of the DR-UV-vis bands corresponding to tetrahedral titanium and octahedral titanium. The experimental absorption bands were fitted taking a sum of Gaussian lines. Three components were considered in the fit: (i) a band at 210 nm , attributed to isolated Ti(IV) species in tetrahedral coordination ; (ii) a band at 260 nm , attributed to titanium in octahedral coordination [40]; and (iii) a band at 310 nm , due to polymeric titanium species grown on the silica surface.

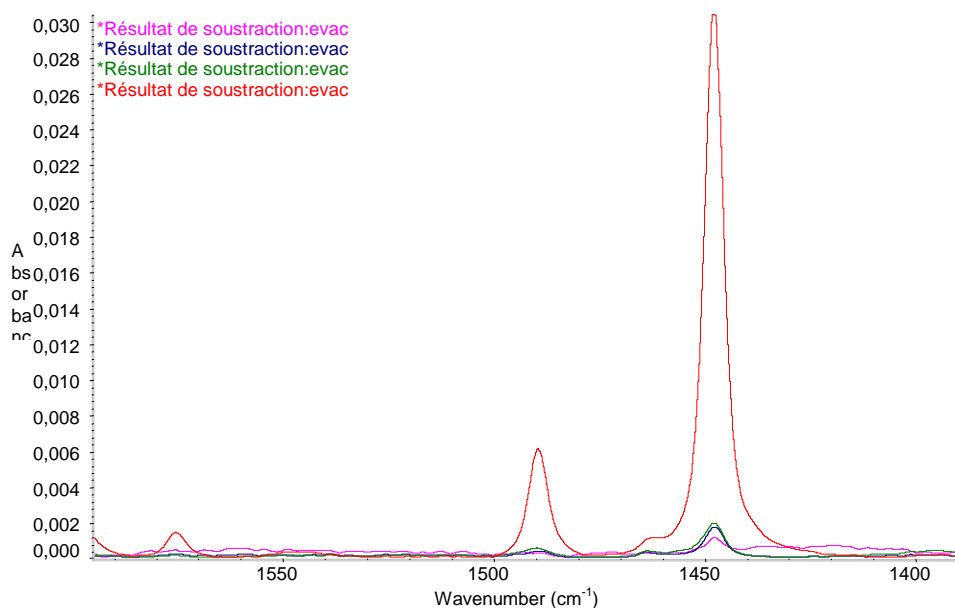
$$T = \frac{S_{(210\text{nm})}}{S_{(260\text{nm})} + S_{(310\text{nm})}} \quad (3)$$



The values (*D*), (*T*) and (*H*) calculated from the deconvoluted peak areas using Eqs. (1-3) are listed in Table 1. At first glance, it is clear that the catalyst calcined at 400 °C presents a higher dispersion than the solids calcined at 250 °C and 600 °C. This observation points to the formation of a larger amount of octahedral coordinated titanium species in solids calcined at 600 °C. The spectra of this catalyst exhibited species at 310 nm (Fig. 3) in a much more intense way than in the other samples. All these findings are in agreement with the UV-vis spectra of the catalysts. Interestingly, the catalyst (calcined at 600 °C) with low titanium dispersion (as derived from the above analysis of the FTIR spectra), also exhibited a low (*T*) ratio (an important contribution of surface polymeric (Ti–O–Ti–O–) titanium species).

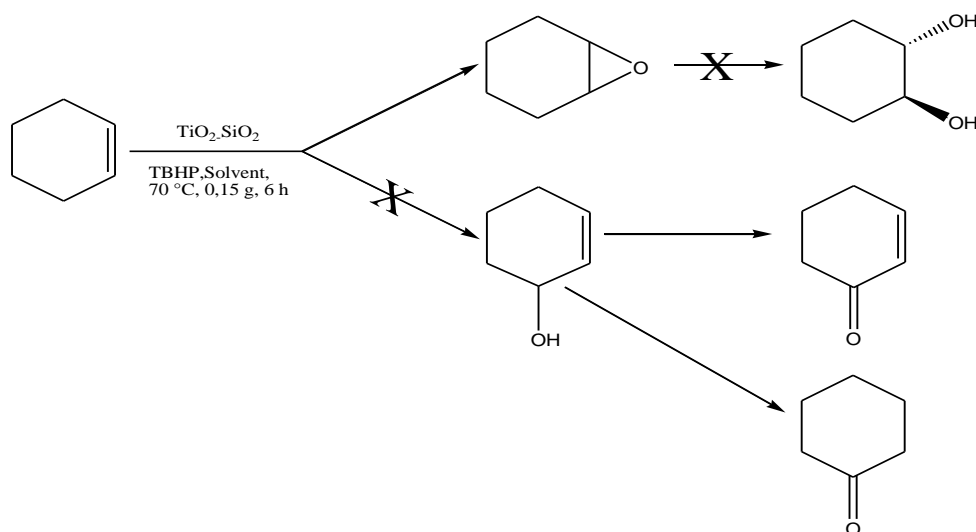
The importance of hydrophobicity of heterogeneous catalysts for selective epoxidation has been emphasized by Sheldon [41]: this will favour the adsorption of nonpolar reactants in competition with polar products, and then will increase both activity and selectivity. The comparison of the separate adsorptions of *n*-hexane and water supported the conclusion that the surface was indeed hydrophobic. It is, however, difficult to measure this property. Weitkamp [42] introduced a hydrophobicity index based on the competitive adsorption of octane and water. Kawai et al [43] evaluated the hydrophobic characteristic by measuring the heat of immersion into water. Percentages of hydrophobicity (*H*), obtained from the deconvoluted peak areas of the $\nu(\text{Si-O-Si})$ band at 1200 cm^{-1} and the OH group at 3440 cm^{-1} , of $\text{TiO}_2\text{-SiO}_2$ mixed oxides activated at different temperatures are shown in Table 1. The hydrophobicity index gradually increases with the activation temperature (250 °C - 400 °C) from 0.39 to 0.51 then decreases to 0.15 at 600 °C.

IR spectra of pyridine adsorption showed the presence of Lewis acid sites (1455 cm^{-1}) in the catalyst 2 wt.% $\text{TiO}_2\text{-SiO}_2$ calcined at 250 °C (Fig 4). We note the absence of characteristic bands of pyridine adsorption on Brønsted acid sites (formation of pyridinium ion leading to two absorption bands at 1545 cm^{-1} and 1637 cm^{-1}). The presence of Lewis acid sites (tetrahedral titanium sites) is responsible for the activity in epoxidation reactions [7 - 8].



Catalytic tests

Epoxidation of cyclohexene, using 2 %TiO₂-SiO₂ prepared catalysts with TBHP, was studied with respect to the peroxide yield. It was observed that cyclohexene was only oxidized to cyclohexene oxide (C6 epoxide), indicating that the selectivity for cyclohexene oxide was almost 100 %, and no other products like cyclohexane diols, cyclohexenol (enol), cyclohexenone (enone), cyclohexanol (ol) and cyclohexanone (one) [15, 44] were detected by GC analysis (Scheme 1). Pure TiO₂ is not active in the epoxidation reaction.



Scheme 1: Mechanism of cyclohexene epoxidation

Effect of calcination temperatures

As shown in Table 1, different calcination temperatures affect the catalytic performance significantly. The catalyst calcined at 250 °C gave moderate epoxide yield, but this yield decreased quickly for the one calcined at 400 °C. When the calcination temperature was increased to 600 °C, the yields increased slightly. These results can be related to the dispersion of titanium ($D_{(Si-O-Ti)}$). It can clearly be seen that the catalyst (600 °C) in which titanium appears as both tetrahedral and polymeric (octahedral) species with low dispersion ($D_{(Si-O-Ti)}$) values exhibited a low epoxide yield [38].

Effect of various solvents

The effects of solvent on the epoxidation of cyclohexene are also depicted in Table 1. These results show a higher epoxide yield when heptane is used as solvent with all catalysts. This solvent has a more significant hydrophobic index compared to tertibutanol and acetonitrile.

For hydrophilic catalysts, the adsorption of reactants is not limited by the retention of hydrophobic solvent heptanes. It is also noted that the epoxide yield decreases (15 % to 6 %) when the calcination temperature increases from 250 °C to 400 °C. This increase is

accompanied by an increase in the hydrophobicity index (0.39 to 0.51). It can thus be concluded that the hydrophobic property is important to this reaction.

Table 1: Catalytic performance of 2 %TiO₂-SiO₂ catalysts in cyclohexene epoxidation

| Entry | catalyst | Calcination °C | Solvent | TBHP addition | Epoxide yield % | H | D | T |
|-------|------------------------------------|----------------|--------------|----------------------|-----------------|------|-------|------|
| 1 | TiO ₂ | 500 | Heptane | At once | 0 | / | / | / |
| 2 | SiO ₂ | 500 | Heptane | At once | 0 | / | / | / |
| 3 | | | Heptane | At once | 15 | | | |
| 4 | | | tertbutanol | At once | 0 | | | |
| 5 | TiO ₂ -SiO ₂ | 250 | Acetonitrile | At once | 0 | 0.39 | 39.95 | 3.18 |
| 6 | | | without | At once | 44 | | | |
| 7 | | | Heptane | Slow | 16 | | | |
| 8 | | | Heptane | At once ^a | 33 | | | |
| 9 | | | Heptane | At once | 6 | | | |
| 10 | | 400 | tertbutanol | At once | 1 | 0.51 | 88.98 | 4.57 |
| 11 | TiO ₂ -SiO ₂ | | Acetonitrile | At once | 0 | | | |
| 12 | | | Heptane | At once | 10 | | | |
| 13 | | 600 | tertbutanol | At once | 0 | 0.15 | 11.21 | 0.71 |
| 14 | | | Acetonitrile | At once | 1 | | | |

(cyclohexene = 37.5 mmol, TBHP = 12.58 mmol, catalyst = 150 mg, Solvent = 4 mL, t = 6 h, T = 75 °C)

a : Anhydrous TBHP

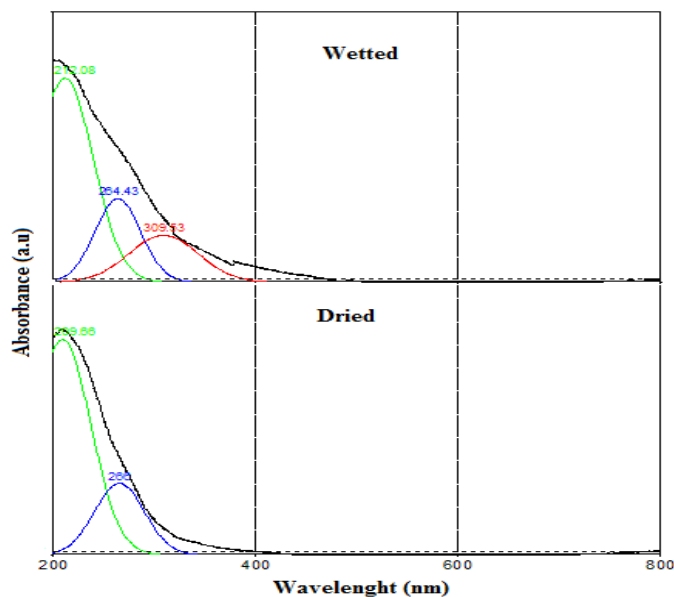
In the presence of tertbutanol as solvent, the epoxidation of cyclohexene did not yield any results, except for the catalyst calcined at 400 °C (1 %) which has the largest hydrophobic index. These results indicate that the catalysts deactivate by pore blocking with polar molecules *t*-butanol, as suggested by the hydrophobicity measurements [45]. In the case of acetonitrile as solvent, the catalyst calcined at 600 °C showed a low epoxide yield (1 %). This low activity may be due to the complexation of Titanium atoms by acetonitrile molecules [7].

Using the system without solvent (Entry 6), an approximately three-fold increase in epoxide yield (44 %) is observed, compared to the system with heptane. The good result obtained in absence of solvent can be attributed to the good access of the organic substrate to the surface of the catalyst.

Effect of slow addition of TBHP

In most papers, the entire oxidant is added at once at the beginning. However, some authors have mentioned the dropwise addition of the oxidant without explaining the purpose of this procedure [46]. In this paper 70 % TBHP was used because of the effect of water on catalyst deactivation; the improvement in activity and selectivity with the slow addition of oxidant was ascribed to the lower amount of water present in the earlier stage of the reaction.

It can be seen that the yield increased slightly (16 %) for the slow addition of TBHP (Entry 7). The positive role of this slow addition may be more related to the lower water content in the reaction mixture than to the lower decomposition. Using anhydrous TBHP (Entry 8) confirms this hypothesis. The catalyst calcined at 250 °C gave a higher yield (33 %). To understand the effect of water on the reaction, a DRS-UV-vis analysis was performed. The catalyst 2 %TiO₂-SiO₂ (250 °C) was dried and then wetted (Figure 5). Both spectra showed a band at 210 nm corresponding to tetrahedral titanium. The deconvolution of the spectrum showed a decrease of the ratio (T) when the catalyst is wetted and become equal to 2.3 (T = 3.18 for the dry catalyst). So, water increased the amount of octahedral titanium, causing catalyst deactivation [12, 21, 22].



CONCLUSION

From the experimental work carried out on the synthesis of TiO₂-SiO₂ catalysts, from their spectroscopic characterization and testing in the liquid-phase epoxidation of cyclohexene with tertibutyl hydroperoxide , the following conclusions can be drawn:

- The UV-Vis DR spectra results of calcined samples confirm the presence of Ti in the form of tetrahedral and octahedral coordination
- The IR spectra of pyridine adsorption showed the presence of Lewis acid sites which are responsible for the activity in epoxidation reactions
- The oxidation reactions of cyclohexene with TBHP as oxidant were 100 % selective toward the formation of epoxide.
- The isolated tetrahedral Ti species are directly connected to the formation of epoxide, whereas the presence of some two-dimensional octahedrally coordinated Ti species is detrimental to epoxide yields.
- The slow addition of oxidant improves the epoxide yield
- Using anhydrous TBHP gave a higher yield (33 %).

REFERENCES

- [1] Iler RK. 1979. The Chemistry of Silica: Solubility, Polymerization, Colloid and Surface Properties and Biochemistry of Silica. Wiley New York
- [2] Brinker CJ, Scherer GW. 1990. Sol-Gel Science: The Physics and Chemistry of Sol-Gel Processing, Academic Press, Boston, MA
- [3] Schubert U. J Chem Soc Dalton Trans 1996: 3343-3348
- [4] Miller J B, Ko E I. Catal Today 1997;35: 269-292
- [5] Pirovano C, Guidotti M, Dal Santo V, Psaro R, Kholdeeva O A, Ivanchikova I D. Catal Today 2012;197:170– 177
- [6] Oki A, Xu Q, Shpeizer B, Clearfield A, Qiu X, Kirumakki S, Tichy S. Catal Commun 2007; 8:950-956
- [7] Cozzolino M, Di Serio M, Tesser R and Santacesaria E. Appl Catal A Gen 2007; 325:256-262
- [8] Notari B. Catal Today 1993; 18:163-172
- [9] Gleeson D, Sankar G, Catlow C R A, Thomas J M, Spano G, Bordiga S, Zecchina A, Lamberti C. Phys Chem Chem Phys 2000; 2: 4812-4817
- [10] Wulff H P. 1975. Patent Shell Oil Company USA
- [11] Hutter R, Mallat T, Baiker A. J Catal 1995;153:177-189
- [12] Hutter R, Mallat T, Baiker A. J Catal 1995; 157:665-675
- [13] Sheldon R A, Vliet MCAV. 2001. Fine chemicals through heterogeneous catalysis Wiley Weinheim
- [14] Mikolajska E, Calvino-Casilda V, Banares M A. Appl Catal A Gen 2012; 421–422: 164–171
- [15] Lahcene D, Choukchou-Braham A, Kappenstein C, Pirault-Roy L J Sol-Gel Sci Technol 2012;64:637–642
- [16] Leus K, Vandichel M, Liu Y Y, Muylaert I, Musschoot J, Pyl S, Vrielinck H, Van Der Voort P. J Catal 2012;285:196–207
- [17] Titinchi S J J, Abbo H S. Catal Today 2013;204:114– 124
- [18] Cai W, Zhou Y, Bao R, Yeu B, He H. Chin J Catal 2013;34:193-199
- [19] Anand C, Srinivasu P, Mane G P, Talapaneni S N, Benzigar M R, Priya S V, Al-deyab S S, Sugi Y, Vinu A. Microporous and Mesoporous Mater 2013;167:146–154
- [20] Gago S, Rodríguez-Borges J E, Teixeira C, Santos A M, Zhao J, Pillinger M, Nunes C D, Petrovski Z, Santos T M, Kühn F E, Romao C C, Goncalves I S. J Mol Catal A Chem 2005; 236:1–6
- [21] Davis R J, Liu Z F. Chem Mater 1997; 9: 2311-2324
- [22] Thomas J M, Sankar G, Klunduk M C, Atfield M P, Maschmeyer T, Johnson B F G, Bell R G . J Phys Chem B 1999;103:8809-8813
- [23] Kung H H, Ko E I. Chem Eng J 1996;64:203-214
- [24] Muller C A, Maciejewski M, Mallat T, Baiker A. J Catal 1999;184: 280–293
- [25] Tchenar Y N, Choukchou-Braham A, Bachir R. Bull Mater Sci 2012; 35(4): 673–681
- [26] Duran A, Serna C, Fornes V, Fernandez-Navarro J M. J Non-Cryst Solids 1986 ; 82:69-77
- [27] Smirnov K S, Graaf B. Microporous Mater 1996;7: 133-138
- [28] Dutoit D C M, Schneider M, Baiker A. J Catal 1995;153:165–176
- [29] Geobaldo F, Bordiga S, Zecchina A, Giannelo E, Leofanti G, Petrini G. Catal Lett 1995;16: 109-115

- [30] Astorino E, Peri J B, Willey R J, Busca G. *J Catal* 1995;157: 482-500
- [31] Deo G, Turek A M, Wach I E, Huybrechts D R C, Jacobs P A (1993) *Zeolites* 13: 365-373
- [32] Henry P F, Weller M T, Wilson C C. *J Phys Chem B* 2001;105: 7452-7458
- [33] Lamberti C, Bordiga S, Zecchina A, Carati A, Fitch A N, Artioli G, Petrini G, Salvalaggio M, Marra G L. *J Catal* 1999;183(2): 222-231
- [34] Gleeson D, Sankar G, Catlow R A, Thomas J M, Spano G, Bordiga S, Zecchina A, Lamberti C. *Phys Chem Chem Phys* 2000;2: 4812-4817
- [35] Fraile J M, García J I, Mayoral J A, Vispe E, Brown D R, Naderi M. *Chem Commun* 2001:1510-1511
- [36] Trong On D, Le Noc L, Bonneviot L. *Chem Commun* 1996:299-307
- [37] Lamberti C, Bordiga S, Arduino D, Zecchina A, Geobaldo F, Spano G, Genoni F, Petrini G, Carati A, Villain F, Vlaic G J. *J Phys Chem B* 1998;102:6382-6390
- [38] Bordiga S, Damin A, Bonino F, Zecchina A, Spano G, Rivetti F, Bolis V, Prestipino C, Lamberti C. *J Phys Chem B* 2002;106:9892-9905
- [39] Capel-Sanchez M C, Campos-Martin J M, Fierro J L G (2003) *J Catal* 217 :195–202
- [40] Notari B. *Adv Catal* 1996;41:253-334
- [41] Sheldon R A, Dakka J. *J Catal Today* 1994;19:215-246
- [42] Berke C H, Kiss A, Kleinschmit P, Weitkamp J. *J Chem Ing Tech* 1991; 63:623-625
- [43] Kawai T, Tsutsumi K. *Colloid Polym Sci* 1992;270:711-715
- [44] EL-Korso S, Rekkab I, Choukchou-Braham A, Bedrane S, Pirault-Roy L, Kappenstein C. *Bull Mater Sci* 2012; 35(7):1187–1194
- [45] Klein S, Thorimbert S, Maier W F. *J Catal* 1996;163: 476–488
- [46] Fraile J M, García J I, Mayoral J A, Vispe E. *Appl Catal A: Gen* 2003; 245:363–376